MODELING & ANALYSIS OF AGS (1998) THERMAL SHOCK EXPERIMENTS

Rusi P. Taleyarkhan, Seokho H. Kim, John R. Haines
Oak Ridge National Laboratory
Oak Ridge, Tennessee, 37831, USA

ABSTRACT

An overview is provided on modeling and analysis of thermal shock experiments conducted during 1998 with high-energy, short-pulse energy deposition in a mercury filled container in the Alternating Gradient Synchrotron (AGS) facility at Brookhaven National Laboratory (BNL). The simulation framework utilized along with the results of simulations for pressure and strain profiles are presented. While the magnitude of peak strain predictions versus data are in reasonable agreement, the temporal variations were found to differ significantly in selected cases, indicating lack of modeling of certain physical phenomena or due to uncertainties in the experimental data gathering techniques. Key thermal-shock related issues and uncertainties are highlighted.

I. INTRODUCTION

In accelerator-driven neutron sources such as the Spallation Neutron Source (SNS) [1] with powers in the 1 MW range (time-averaged), the interaction of the energetic proton beam with the mercury target can lead to very high heating rates in the target. Although the resulting temperature rise is relatively small (a few °C), the rate of temperature rise is enormous (~10^7 °C/s) during the very brief beam pulse (~0.5s). The resulting compression of the mercury leads to the production of large amplitude pressure waves in the mercury that interact with the walls of the mercury target and the bulk flow field. Understanding and predicting propagation of pressure pulses in the target (either liquid or solid) are considered critical for establishing the feasibility of constructing and safely operating such devices. Along with other objectives, in order to develop a code validation and benchmarking database, a collaborative arrangement was set up[2] to conduct experiments with close to full-scale target chambers filled with mercury subjected to (as close-to prototypic) short-pulse energy pulses. The AGS facility at Brookhaven National Laboratory (BNL) was chosen to conduct these experiments.

Specific experiments conducted at BNL's AGS facility during 1998 (the subject of this paper) involved high-energy (24 GeV) proton energy deposition in the mercury target over a time frame of ~ 0.1s. The target consisted of an ~ 1 m. long cylindrical stainless steel shell with a hemispherical dome at the leading edge. It was filled with mercury at room temperature and pressure. Several optical strain gages were attached to the surface of the steel target. Figure 1 shows a schematic representation of the test vessel along with the main dimensions and positions of three optical strain gages at which meaningful data were obtained. As opposed to data taken during 1997, these tests included strain gages in the hemispherical dome region. The proton pulse shape was roughly parabolic and was estimated to be of ~ 0.05 m in radius. Details of the estimated pulse shape and spatial variation are provided elsewhere[2]. This paper provides a perspective overview of ongoing modeling and analysis work related to the above-mentioned experiment in which about 7-9 kJ of thermal energy was deposited into the mercury-filled target over 0.1s.

II. MODELING AND ANALYSIS FRAMEWORK

The CTH code system[3] was used as a basis for developing the appropriate simulation framework. CTH is a three-dimensional (3-D), shock-physics code, sometimes loosely referred to as a hydrocode. This code and associated technology base have been used extensively to simulate explosive processes (such as molten metal-water vapor explosions, and hydrogen detonation) in enclosed fluid-structure systems.[4-6] It is now being adopted[7] for characterizing the current thermal-shock process in a coupled manner,

simultaneously accounting for localized compression pulses from rapid heat deposition, the transport of the compression wave through the mercury, interaction of this wave with the surrounding structure, feedback to the mercury from these structures, and multi-dimensional reflection patterns including rarefaction-induced material fracture (i.e., cavitation in fluids).

Modeling and analysis work are being performed in several areas. Modeling is conducted in a staged manner starting with a simple two-dimensional (2-D) geometry, followed by full-scope 3-D model development (using CTH by itself, or combining it's core capabilities with a finite-element structural mechanics code).

Although the geometry of the AGS experiment target has some three-dimensional features (e.g., flanges, supports, fill tube), it was deliberately designed to remain as two-dimensional as possible. As a first cut, a 2-D model was built using CTH with cylindrical symmetry. This model is shown in Figure 1 in which key dimensions are depicted along with locations of key tracer points (in the fluid and shell).

The following key assumptions were made:

1. Mercury and steel interfaces will be characterized by perfect contact. This assumption was necessary to permit modeling to proceed, although it is recognized that imperfect contact (with a mercury-gas layer) between mercury and steel is a distinct possibility. This is one of the key attributes necessary for successful depiction of complex fluid-structural behavior. The interface between steel and fluid is characterized by the absence of strength in mixed (fluid-steel) cells.

2. The Mie-Gruniesen (MG) equation-of-state (EOS) adequately represents the mercury liquid in compression and tensile states. The MG-EOS is well-known to be useful for use for materials in the compression state. It is recognized, however, that extension to tensile states may not be adequate, especially when gaseous or vaporous cavitation may occur below a certain pressure threshold.

3. Cavitation effects are negligible. This is a key presumption, since clear-cut evidence exists to indicate cavitation in mercury (without degassing) can take place at relatively modest tensile pressures (see companion paper by F. Moraga and R. P. Taleyarkhan)[8].

4. Thermal energy transfer from mercury to the steel is negligible. This assumption is valid for the relatively short duration (~ 300 microseconds) of time for thermal shock studies reported herein. It is recognized, however, that for longer duration approaching the time constant of the shell structures, thermal energy transfer will need to be accounted for.

The energy deposition profile used for simulation was taken from Ref. 2. Since CTH requires energy deposition to be introduced in discrete material regions, the profile of Ref. 2, was divided into 5 radial and 10 axial zones. About 7 kJ of thermal energy is deposited in the mercury and steel over 100 nanoseconds. A total of ~68,000 cells were used to represent the AGS target and surroundings. Tracer points were attached to the steel shell at selected locations (where strain gages were positioned). Additional tracer points were introduced in the steel and mercury to assess wave propagation phenomena along with the assessment of variations in shear stresses at key locations.

III. RESULTS OF SIMULATIONS

Selected results of simulations are shown in Figures 2 through 7. The locations for these transient variations of pressure and strain values are indicated in Figure 1. As noted in Figure 1, the locations of optical strain gages #18&19, #9&10, and #3 coincide with Lagrangian tracer points L22, L25 and L28, respectively.

As was already mentioned in an earlier comparison, it is seen from Figure 2 that negative pressures in mercury imply that mercury can support a rarefaction process. This result is an artifact of assuming a solid-like equation-of-state (EOS) for mercury and the presumption that liquid mercury will not cavitate. It is realized that simulation of more realistic physics of cavitation and geometry are required to improve our understanding and predictive capabilities. It is also seen from Figures 2 & 3 that, for the geometry under investigation, tensile fluid pressures will vary from ~ -20 MPa in the central regions (see trace for L3) to between ~ -6 MPa (for L4 next to the front window) and ~ -1 MPa at the side wall regions (see pressure trace for L6). Comparing these values with data taken in the past it is apparent that cavitation of mercury can not be ruled out, neither in the bulk region, nor at the mercury-steel interfaces. However, the intensity of cavitation near steel walls is clearly greater for the fluid in the front window region than at the side walls (where most of the strain gages were located).

Figures 4, 5 & 7 present predicted versus measured strain values at L22, L25 and L28 tracer points corresponding to locations for gages #18&19, #9&10 and #3, respectively. The three different measured values at the same locations are plotted for comparison against the predictions in figures. As can be clearly seen, in all cases except for L28, the magnitude of strain predicted is reasonably close to that recorded in the experiments. For example, at L22 (Figure 4) the monitored magnitude of

circumferential strain varied between +9 to -4 microstrain. The predictions are between +20 to ~ -10 microstrain. Also seen from Figure 5, the predicted longitudinal strain at L25 varies between +20 and -18 microstrain while the measurement is between +28 and -20 microstrain. It is seen in the figures that substantial discrepancies exist in the overall transient profile between the predictions and the measurements. As seen in Figures 4 & 5, peaks and valleys in strain value occur with a different frequency. These discrepancies between the measurement and the predictions may be because of several reasons. One of them could be a lack of cavitation modeling in the predictions while cavitation onset is certain based on pressure predictions as seen in Figures 2 & 3. It is observed in the measurements that two optical gauges located side by side (i.e., #18 & #19, and #9 & #10) gave substantially different readings. Also, it is seen that the readings vary substantially from one test measurement to another.

The predicted longitudinal strain at L25 is compared against the hoop strain at the same location in Figure 6. It is interesting to note that the hoop stain is twice as large as the longitudinal strain, and its transient behavior and size are closer to those of the measured longitudinal strain as shown in Figure 5.

Figure 7 presents results for longitudinal strain at L28 (gage #3). As noted therein, the measurements seem to indicate that the stress wave has been largely dissipated at this location which is only ~15cm downstream from L25, whereas the predicted strain is still substantial as shown in Figure 5. It is strongly suspected that gage #3 was providing erroneous values during measurements (due to possible mechanical problems).

It should be noted that, the above-mentioned comparisons were made without accounting for onset of cavitation in the mercury fluid. As already mentioned, recent data (see companion paper by F. Moraga and R. P. Taleyarkhan) indicate the onset threshold for cavitation at tensile pressures of less than -1 MPa. Scoping simulations conducted (but not reported herein) indicate a significant change in predicted strain spectra (especially with time) when cavitation onset is allowed - especially at locations close to the front window where the proton beam strikes the mercury filled chamber. As may be expected, the degree of cavitation and resulting spectrum of pressure pulsation in the mercury and the steel shell structure will vary with position.

Another point of caution concerns the science of making appropriate comparisons. The predictions of strain from a computer code against strain gage data should be made with due caution, especially when comparing against longitudinal strain values in a body with cylindrical symmetry. A strain gage monitors variations in separation between two "glued" points, whereas, computer code predictions arise out of the strain tensor for a given cell or node. Minor differences in epoxy performance (or lack of it) may present unusual differences in monitored strain, which may account for the highly different transient variations seen between strain gages #18 and #19 (which were very close together). For a body with cylindrical symmetry, it is far more appropriate and straightforward to compare circumferential strain (due to absence of variations in the azimuthal direction). However, this point must be tempered somewhat, since practical problems and uncertainties emanate when positioning optical strain gages around curvilinear surfaces.

IV. SUMMARY AND CONCLUSION

To summarize, preliminary assessments for thermal shock in the cylindrical mercury target used in the AGS experiment have indicated reasonably good agreement between predictions and data. Peak strain magnitudes agree reasonably well with those observed experimentally. However, the transient variations in pulse shape did not agree in all cases. It is not clear what degree of uncertainty exists in the data gathering technique itself, or if three-dimensional effects played a significant role (since the target assembly does incorporate a series of instrumentation taps and flanges). Based on recent experimental evidence, it appears that cavitation in the mercury should have played a significant role in terms of modifying the time-varying shape of strain measurements.

REFERENCES

1. T. A. Gabriel, et. al., "Overview of the SNS Target Station," *Proc. of International Topical Meeting on Advanced Reactor Safety*, ARS'97, Orlando, Florida (1997).
2. G. S. Bauer et al., "Heat Deposition in the Mercury Target," 2nd General Planning Meeting of the AGS-Spallation Target Experiment Collaboration," Paris, September 25-26 (1997).
3. J. M. McGlaun and S. L. Thompson, "CTH: A Three-Dimensional Shock-Wave Physics Code," International Journal of Impact Engineering, Vol. 10, p.251-360 (1990).
4. V. Georgevich and R. P. Taleyarkhan, "Deterministic Method of Evaluating Multidimensional Explosive Loads Generated by Fuel Coolant Interaction in Uranium-Aluminum Fueled Reactors," *Transaction, Annual American Nuclear Society Conference*, November 14-19 (1993).

5. R. P. Taleyarkhan, et. al., "Analysis and Modeling of Flow-Blockage Induced Steam Explosion Events in the High Flux Isotope Reactor," *Nuclear Safety Journal*, Jan.-June (1994).
6. R. P. Taleyarkhan, et. al., "Modeling and Analysis of Hydrogen Detonation Events in the Advanced Neutron Source Reactor Containment," *Proc. Third International Conference on Containment Design and Operation*, Toronto, Canada (1994).
7. R. P. Taleyarkhan, et al., "Thermal Shock Assessments for the SNS Target System," *Proc. of Intl. Topical Meeting on Advanced Reactor Safety (ARS'97)*, Orlando, Florida, June 1-5 (1997).
8. F. Moraga, and R. P. Taleyarkhan, "Static and Transient Cavitation Threshold Measurements in Mercury," *Proc. of the 3rd Intl. Topical Meeting on Accelerator Applications (AccApp'99)*, Long Beach, CA, USA, November (1999).

Disclaimer

This work was performed as part of the AGS Spallation Target Collaboration (ASTE). The ASTE collaboration has been performed between several US, European, and Japanese laboratories, to carry out a test program at BNL's AGS facility.

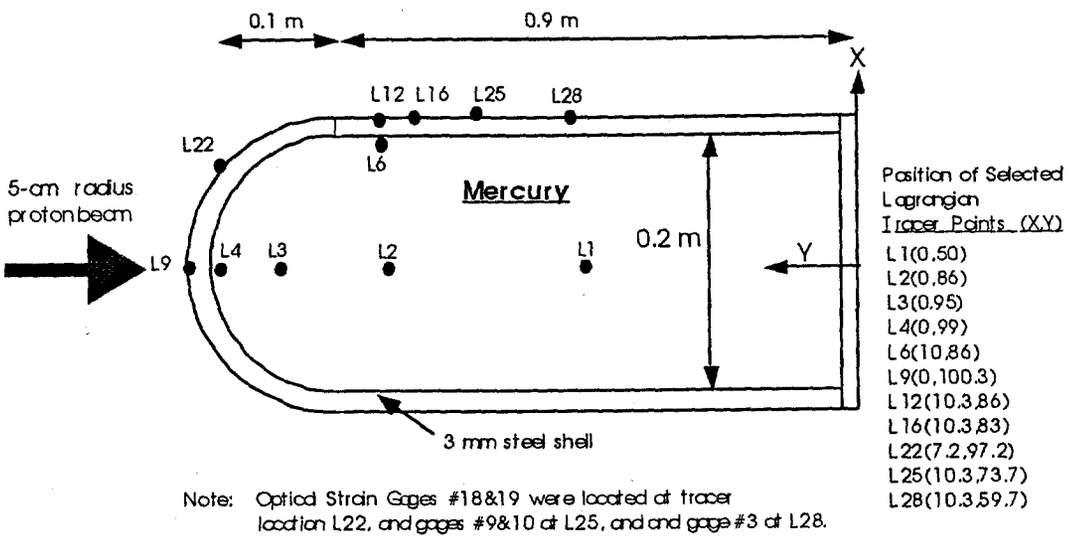

Figure 1. Schematic Representation of Mercury-Filled Test Vessel Used in AGS Experiments & Location of Optical Strain Gage Sensors.

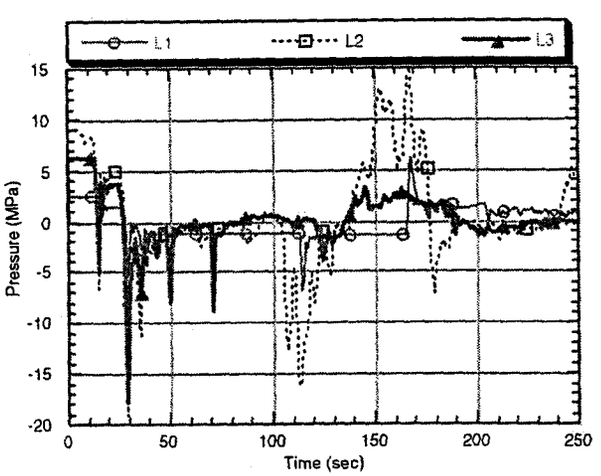

Figure 2. Predicted Pressure Variations in Mercury at the Location #L1, L2, and L3.

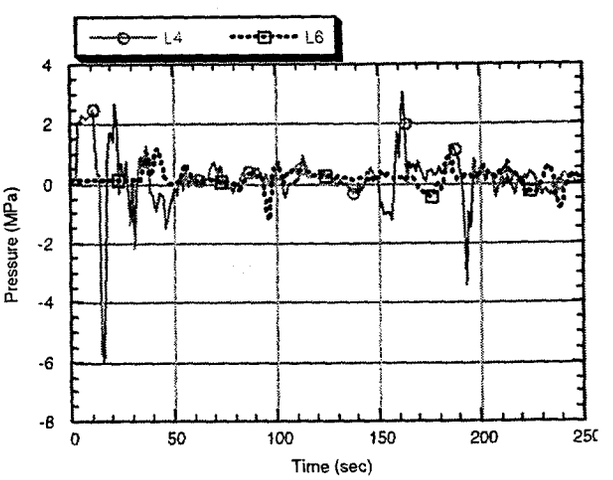

Figure 3. Predicted Pressure Variations in Mercury at the Location #L4 and L6 (near the wall).

Taleyarkhan KIM HAINES 4

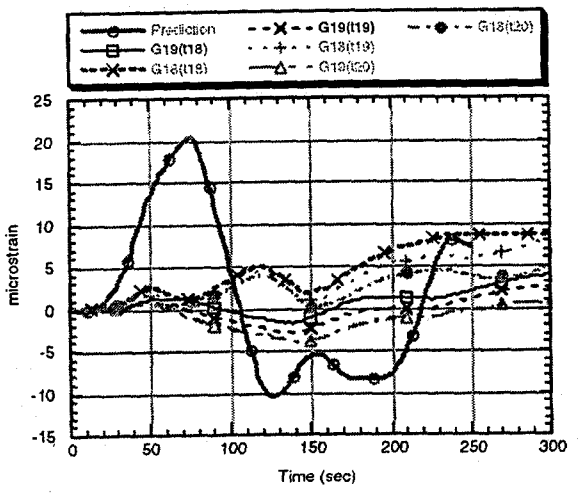

Figure 4. Predicted Vs Measured Circumferential Strains at L22 (Gages #18 & 19 of Various Tests)

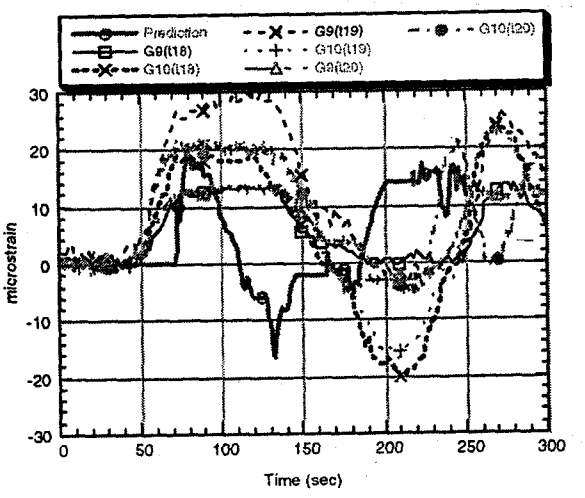

Figure 5. Predicted Vs Measured Longitudinal Strains at L25 (Gages #9 & 10 of Various Tests)

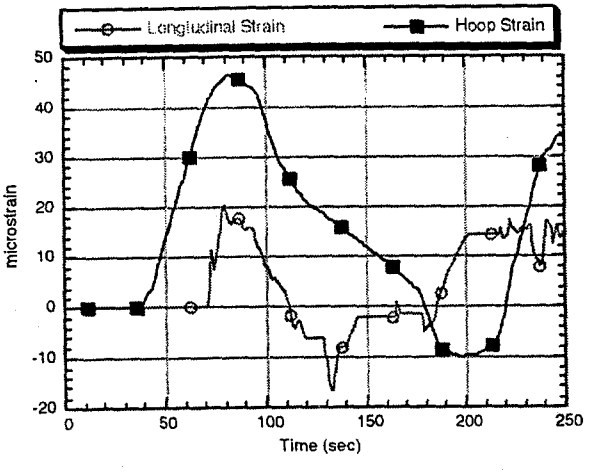

Figure 6. Predicted Longitudinal Strain Vs Hoop Strain at L25

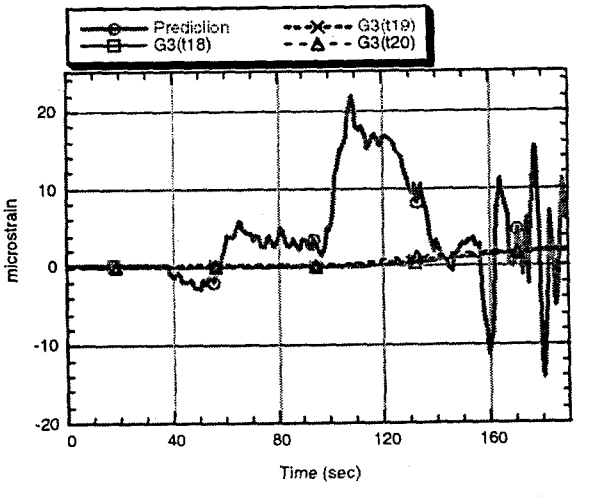

Figure 7. Predicted Vs Measured Longitudinal Strains at L28 (Gage #3 of Various Tests)